NTNU
Kunnskap for en bedre verden

Department of Mathematical Sciences

TMA4212 - Numerical solution of differential equations by difference methods

Galerkin Approximation for Solution of PDE for Fluid Behaviour

Authors:
Peder Brekke
Simen Nesland
Espen Bjørge Urheim

26.03.2023

1 Introduction

The aim of this paper is to investigate a partial differential equation describing the behavior of a convective and diffusive substance. We start by establishing the existence and uniqueness of a solution to the equation. Then, we proceed to implement a $\mathbb{P}_1$ finite element method and perform a numerical analysis of the problem, examining the convergence rates of both smooth and non-smooth solutions. Here we found an analytic error bound for twice differentiable functions, also showing numerical test where this bound is upheld. For non-smooth functions a clear error bound was not found. Lastly, we investigated the impact of the node distribution on the accuracy of the finite element method. Here we experimented with multiple different node distributions.

2 Analyzing the problem

The 1d stationary convection diffusion problem we will look at is

$$-\partial_x(\alpha(x)\partial_x u) + \partial_x(b(x)u) + c(x)u = f(x) \quad \text{in} \quad \Omega = (0,1), \tag{1}$$

where $\alpha(x) > 0$ is the diffusion coefficient, $b(x)$ is fluid velocity, $c(x) > 0$ is the decay rate of the substance and $f(x)$ defines a source of flow. Here we assume $\alpha \geq \alpha_0 > 0$, $c > 0$, that $\|\alpha\|_{L^\infty} + \|b\|_{L^\infty} + \|c\|_{L^\infty} + \|f\|_{L^2} \leq K$, and that $u(0) = 0 = u(1)$. In this first section we will study the problem analytically, with the goal of proving existence of a solution.

2.1 A weak formulation

We start by finding a new way of formulating the problem. Multiplying (1) by $v \in H_0^1(0,1)$ (implying v satisfies $v(0) = 0 = v(1)$), and integrating by parts, we find

$$\begin{aligned} a(u,v) &= \int_0^1 -\partial_x(\alpha u_x)v + \partial_x(bu)v + cuv\,dx \\ &\overset{\text{ibp}}{=} [-\alpha u_x v + buv]_0^1 - \int_0^1 (-\alpha u_x v_x + buv_x - cuv)\,dx = \int_0^1 (\alpha u_x v_x - buv_x + cuv)\,dx \end{aligned}$$

with the corresponding right hand side $F(v) = \int_0^1 fv\,dx$. This shows that any classical solution u of (1) satisfies

$$a(u,v) = F(v) \quad \forall\, v \in H_0^1(0,1). \tag{2}$$

2.2 Existence of a solution

To prove that a unique solution u of (2) actually exists, we need to show that $a(u,v)$ is bilinear, continuous and coercive, and that $F(v)$ is a bounded linear functional. We start by proving bilinearity of a. Since the differential operator is linear, we find that

$$\begin{aligned} a(c_1u_1 + c_2u_2, v) &= \int_0^1 (\alpha\partial_x(c_1u_1 + c_2u_2)v_x - b(c_1u_1 + c_2u_2)v_x + c(c_1u_1 + c_2u_2)v)\,dx \\ &= c_1\int_0^1 (\alpha\partial_x u_1 v_x - bu_1 v_x + cu_1 v)\,dx + c_2\int_0^1 (\alpha\partial_x u_2 v_x - bu_2 v_x + cu_2 v)\,dx \\ &= c_1 a(u_1,v) + c_2(u_2,v) \end{aligned}$$

and analogously $a(u, c_1v_1 + c_2v_2) = c_1a(u, v_1) + c_2(u, v_2)$, which proves bilinearity.

Next we show that $a(u, v)$ is a continuous form on $H^1 \times H^1$, i.e. that $a(u, v) \leq M\|u\|_{H^1}\|v\|_{H^1}$ for all $u, v \in H_0^1$. For this we use that α, b and c are bounded in L^∞, the Cauchy-Schwarz inequality and the H^1-norm, $\|u\|_{H^1}^2 = \|u\|_{L^2}^2 + \|u_x\|_{L^2}^2 \Rightarrow \|u\|_{L^2}, \|u_x\|_{L^2} \leq \|u\|_{H^1}$.

$$\begin{aligned} a(u,v) &= \int_0^1 \alpha u_x v_x \, dx + \int_0^1 (-buv_x) \, dx + \int_0^1 cuv \, dx \\ &\leq \max_{x\in(0,1)} |\alpha(x)| \cdot \langle u_x, v_x \rangle_{L^2} + \max_{x\in(0,1)} |b| \cdot \langle u, v_x \rangle_{L^2} + \max_{x\in(0,1)} |c| \cdot \langle u, v \rangle_{L^2} \\ &\overset{\text{CS}}{\leq} \|\alpha\|_{L^\infty}\|u_x\|_{L^2}\|v_x\|_{L^2} + \|b\|_{L^\infty}\|u\|_{L^2}\|v_x\|_{L^2} + \|c\|_{L^\infty}\|u\|_{L^2}\|v\|_{L^2} \\ &\leq (\|\alpha\|_{L^\infty} + \|b\|_{L^\infty} + \|c\|_{L^\infty}) \cdot \|u\|_{H^1}\|v\|_{H^1} = M\|u\|_{H^1}\|v\|_{H^1}. \end{aligned}$$

Thus we have proven continuity of $a(u, v)$ with constant $M = \|\alpha\|_{L^\infty} + \|b\|_{L^\infty} + \|c\|_{L^\infty}$.

Next we prove that $F(v)$ is a linear and continuous (bounded) functional on H^1. Linearity is easy to show,

$$F(c_1v_1 + c_2v_2) = \int_0^1 f \cdot (c_1v_1 + c_2v_2) \, dx = c_1 \int_0^1 fv_1 \, dx + c_2 \int_0^1 fv_2 \, dx = c_1F(v_1) + c_2F(v_2).$$

To prove continuity we use Cauchy-Schwarz,

$$|F(v)| \leq \|f\|_{L^2}\|v\|_{L^2} \leq \|f\|_{L^2}\|v\|_{H^1}.$$

Hence, by the assumption that f is bounded in L^2, we conclude that $F(v)$ is bounded.

The last step to prove existence of a solution of (2) is to show coercivity of $a(u, v)$. As a first step to do so, we prove that the Gårding inequality holds for $a(u, v)$. Using properties of the absolute value, since the second term is negative, we have

$$a(u,u) = \int_0^1 (\alpha u_x^2 - buu_x + cu^2) \, dx \geq \int_0^1 (\alpha u_x^2 - |b||uu_x| + cu^2) \, dx.$$

Here we use Young's inequality to argue that $uu_x \leq \frac{1}{2\varepsilon}u^2 + \frac{\varepsilon}{2}u_x^2$ for all $\varepsilon > 0$. Since $|b| > 0$ and $\frac{1}{2\varepsilon}u^2 + \frac{\varepsilon}{2}u_x^2 \geq 0$, we conclude that

$$\begin{aligned} a(u,u) &\geq \int_0^1 (\alpha u_x^2 - |b|(\frac{1}{2\varepsilon}u^2 + \frac{\varepsilon}{2}u_x^2) + cu^2) \, dx \\ &= (\alpha - \frac{\varepsilon}{2}|b|) \int_0^1 v_x^2 \, dx + (c - \frac{1}{2\varepsilon}|b|) \int_0^1 v^2 \, dx \end{aligned} \tag{3}$$

Next we prove that $a(u, v)$ is coercive, i.e. that $a(v, v) \geq \gamma\|v\|_{H^1}^2$ for some $\gamma > 0$. To do so we use (3), from which we know that

$$\begin{aligned} a(v,v) &\geq (\alpha - \frac{\varepsilon}{2}|b|) \int_0^1 u_x^2 \, dx + (c - \frac{1}{2\varepsilon}|b|) \int_0^1 u^2 \, dx = (\alpha - \frac{\varepsilon}{2}|b|)\|v_x\|_{L^2}^2 + (c - \frac{1}{2\varepsilon}|b|)\|v\|_{L^2}^2 \\ &\geq \min\{\alpha - \frac{\varepsilon}{2}|b|, \, c - \frac{1}{2\varepsilon}|b|\} \cdot (\|v_x\|_{L^2}^2 + \|v\|_{L^2}^2) = \min\{\alpha - \frac{\varepsilon}{2}|b|, \, c - \frac{1}{2\varepsilon}|b|\}\|v\|_{H^1}^2. \end{aligned}$$

Since we require $\gamma > 0$, we must have that 1) $\alpha - \frac{\varepsilon}{2}|b| > 0 \Rightarrow \varepsilon < \frac{2\alpha}{|b|}$ and 2) $c - \frac{1}{2\varepsilon}|b| > 0 \Rightarrow c - \frac{|b|^2}{2\cdot 2\alpha} > 0 \Rightarrow c > \frac{|b|^2}{4\alpha}$ for coercivity. Thus, when $c > \frac{|b|^2}{2\alpha}$, $a(u, v)$ is coercive.

Since $a(u,v)$ is bilinear, continuous and coercive when $c > \frac{|b|^2}{4\alpha}$, and since $F(v)$ is linear and continuous, we conclude by the Lax-Milgram theorem that, in this case, there exists a unique solution $u \in H_0^1(0,1)$ such that $a(u,v) = F(v)$ for all $v \in H_0^1(0,1)$. □

Formulated differently, we have now confirmed that there exists a solution to the problem

$$\text{Find } u \in H_0^1(0,1) \text{ such that} \quad a(u,v) = F(v) \quad \forall\, v \in H_0^1(0,1). \tag{V}$$

3 Solving (V) with a $\mathbb{P}_1$ FEM

We will now attempt to solve (V) with a $\mathbb{P}_1$ finite element method. This means that we will solve the Galerkin approximation,

$$\text{Find } u_h \in V_h \text{ such that} \quad a(u_h, v_h) = F(v_h) \quad \forall\, v_h \in V_h, \tag{V_h}$$

where $V_h = X_h^1(0,1) \cap H_0^1(0,1)$ is the finite-dimensional subspace of the Hilbert space $H_0^1(0,1)$ that only consists of functions that are continuous and piecewise linear on a grid on $\Omega = (0,1)$. We start with assembly and implementation.

3.1 Assembly and implementation

To solve (V_h), the Galerkin approximation, we use the common basis for piecewise linear functions, the hat functions (Section 2.2, Curry 2018). These are described by

$$\varphi_i(x) = \begin{cases} \frac{x - x_{i-1}}{x_i - x_{i-1}}, & x_{i-1} < x \leq x_i \\ \frac{x_{i+1} - x}{x_{i+1} - x_i}, & x_i < x \leq x_{i+1} \\ 0, & \text{else} \end{cases} \tag{4}$$

Using this finite basis, our problem of finding u_h turns into finding coefficients for the basis. This is just a linear problem and can be written as $A\boldsymbol{U} = \boldsymbol{F}$ where we are looking for $\boldsymbol{U}$. It can be shown that in this equivalent problem, the so-called stiffness matrix A is described by

$$\begin{aligned} A_{ij} = a(\varphi_i, \varphi_j) &= \int_0^1 (\alpha \varphi_i' \varphi_j' - b\varphi_i \varphi_j' + c\varphi_i \varphi_j) dx \\ &= \sum_k \alpha \int_{x_k}^{x_{k+1}} \varphi_i' \varphi_j' dx - b \int_{x_k}^{x_{k+1}} \varphi_i \varphi_j dx + c \int_{x_k}^{x_{k+1}} \varphi_i \varphi_j dx \end{aligned}$$

Studying this expression we find that this will be zero for all cases, except for $j \in \{i-1, i, i+1\}$. This becomes obvious by looking at (4), as we need both functions to be different from zero on the interval we are studying. The non-zero entries are easily derived by computing the integrals, using (4). The results describing the diagonal and the two off-diagonals are summarized in Table 1.

To solve the linear system we also have to compute $\boldsymbol{F}$. Just as for A it can be shown that in the Galerkin approximation we have

$$\boldsymbol{F}_i = \int_0^1 f \cdot \varphi_i dx.$$

	α-term	b-term	c-term
$j = i - 1$	$-\frac{1}{h_i}$	$\frac{1}{2}$	$\frac{h_i}{6}$
$j = i$	$\frac{1}{h_i} + \frac{1}{h_{i+1}}$	0	$\frac{h_i + h_{i+1}}{3}$
$j = i + 1$	$-\frac{1}{h_{i+1}}$	$-\frac{1}{2}$	$\frac{h_{i+1}}{6}$

Table 1: The results of the integrals to compute A.

It is clear that in this case we also get mostly zeros, and for a given i we only have to consider the interval (x_{i-1}, x_{i+1}). On this interval we can use a numerical quadrature, and we have opted for SciPy's implementation of Simpson's rule.

After constructing A and $\boldsymbol{F}$ we are ready to solve the system. We do this using SciPy's "sparse.linalg.spsolve()" and finally adding the boundaries (0 in our case). It is worth noting that given an M-interval system we have $M + 1$ nodes, but we are only solving a $(M - 1) \times (M - 1)$ system because we have the boundary conditions. Two different solutions are given in Figure 2.

```
A=
 [[ 20.07  -9.48   0.     0.     0.     0.     0.     0.     0.  ]
 [-10.48  20.07  -9.48   0.     0.     0.     0.     0.     0.  ]
 [  0.   -10.48  20.07  -9.48   0.     0.     0.     0.     0.  ]
 [  0.     0.   -10.48  20.07  -9.48   0.     0.     0.     0.  ]
 [  0.     0.     0.   -10.48  20.07  -9.48   0.     0.     0.  ]
 [  0.     0.     0.     0.   -10.48  20.07  -9.48   0.     0.  ]
 [  0.     0.     0.     0.     0.   -10.48  20.07  -9.48   0.  ]
 [  0.     0.     0.     0.     0.     0.   -10.48  20.07  -9.48]
 [  0.     0.     0.     0.     0.     0.     0.   -10.48  20.07]]
```

Figure 1: Example of stiffness-matrix A. This one is calculated given parameters/RHS given for the left plot in Figure 2. Note that this is actually a reduced matrix, i.e. without the first and last column and row. Thus it is $(M - 1) \times (M - 1) = 9 \times 9$.

After testing the implementation for a couple of examples we impose an exact solution to test the convergence rate. Using $u(x) = \sin(3\pi x)$ and inserting into (V) we find

$$f(x) = 9\pi^2 \alpha \sin(3\pi x) + 3b\pi \cos(3\pi x) + c \sin(3\pi x).$$

Using this f as the RHS, we compute a numerical solution using our implementation for different values of M, i.e. variable number of subintervals and hence variable stepsize. For the different stepsizes we then compute the L_2 and H^1 norm of the error and produce log-log plots. The results are shown in Figure 3. Clearly the order is 2 in the L_2 norm and 1 in the H^1 norm.

3.2 Analytic error analysis

To compare the numerical results to theory, we will now derive an error bound in H^1.

Let u and u_h be solutions of the infinite and finite dimensional problems (V) and (V_h), respectively, and let $v_h \in X_h^1(0,1) \cap H_0^1(0,1)$. Since $a(u, v)$ is bilinear and v_h also is in $H_0^1(0,1)$, we have that

$$a(u - u_h, v_h) = a(u, v_h) - a(u_h, v_h) = F(v_h) - F(v_h) = 0,$$

which proves Galerkin orthogonality.

We know from earlier sections that $a(u,v)$ is bilinear, continuous and coercive with constants M and γ, that the Lax-Milgram theorem holds and that Galerkin orthogonality is satisfied. This means that Cea's lemma also holds,

$$\|u-u_h\|_{H^1} \leq \frac{M}{\gamma} \inf_{v_h \in X_h^1 \cap H_0^1} \|u-v_h\|_{H^1}.$$

Now let v_h be the piecewise continuous polynomial of degree one that interpolates u, i.e. $v_h = I_h u$, which is in $X_h^1 \cap H_0^1$. We then end up with the error bound

$$\|e_h\|_{H^1} = \|u-u_h\|_{H^1} \leq \frac{M}{\gamma}\|u-I_h u\|_{H^1} \leq \frac{2M}{\gamma}\|u_{xx}\|_{L^2(0,1)} \cdot h \tag{5}$$

where $M = \|\alpha\|_{L^\infty} + \|b\|_{L^\infty} + \|c\|_{L^\infty}$ and $\gamma = \min\{\alpha - \frac{\varepsilon}{2}|b|,\, c - \frac{1}{2\varepsilon}|b|\}$ with $c > \frac{|b|^2}{2\alpha}$, and where h denotes the maximum step length in the grid. It is important to note that for this error bound we assume u to be twice differentiable, which may not be the case. For the previous section however, with $u(x) = \sin(3\pi x)$, the bound is valid.

We see from Figure 3 that the numerical convergence is consistent with the derived error bound, i.e. linear convergence in H^1-norm. The quadratic convergence in L^2 is also coherent with theory, although we will not derive the result here.

3.3 Testing with a non-smooth u

We will now test our $\mathbb{P}_1$ FEM on non-smooth solutions. For this we introduce two new functions,

$$w_1(x) = \begin{cases} 2x, & x \in (0, \frac{1}{2}) \\ 1-2x, & x \in (\frac{1}{2}, 1) \end{cases} \quad \text{and} \quad w_2(x) = x - |x|^{\frac{2}{3}},$$

We use the definition of a weak derivative, $\int_0^1 w_i'(x)v(x)\,dx = -\int_0^1 w_i(x)v'(x)$ for all $v \in H_0^1(0,1)$, and apply i.b.p. to find

$$w_1'(x) = 2 - 4\theta(x-\frac{1}{2}), \quad \theta(x) = \begin{cases} 0, & x \leq 0, \\ 1, & x > 0, \end{cases} \quad \text{and} \quad w_2'(x) = 1 - \frac{2}{3x^{\frac{1}{3}}}, \quad x \in (0,1).$$

This means that $w_1(x)$ is not differentiable at $x = \frac{1}{2}$, which is easy to see as it is a hat function, and $w_2(x)$ is not differentiable at $x = 0$ as the derivative is not defined here. We know that the Dirac delta function $\delta(x) \notin L^2(0,1)$ is the weak derivative of the Heaviside function $\theta(x)$. Using the definition of weak derivative the same way, we find that $w_2''(x) = \frac{2}{9}x^{-\frac{4}{3}}$. Taking the L^2-norm, we find

$$\|w_1\|_{L^2(0,1)}^2 = \int_0^{\frac{1}{2}} |2x|^2\,dx + \int_{\frac{1}{2}}^1 |1-2x|^2\,dx = \frac{1}{3} < \infty \Rightarrow w_1 \in L^2$$

$$\|w_1'\|_{L^2(0,1)}^2 = \int_0^{\frac{1}{2}} |2|^2\,dx + \int_{\frac{1}{2}}^1 |-2|^2\,dx = 4 < \infty \Rightarrow w_1' \in L^2$$

$$\|w_2\|_{L^2(0,1)}^2 = \int_0^1 |x-|x|^{\frac{2}{3}}|^2\,dx = \frac{1}{84} < \infty \Rightarrow w_2 \in L^2$$

$$\|w_2'\|_{L^2(0,1)}^2 = \int_0^1 |1-|x|^{-\frac{1}{3}}|^2\,dx = \frac{1}{3} < \infty \Rightarrow w_2' \in L^2$$

$$\|w_2''\|_{L^2(0,1)}^2 = \lim_{k\to 0} \int_k^1 |\frac{2}{9}x^{-\frac{4}{3}}|^2\,dx \to \infty \Rightarrow w_2'' \notin L^2.$$

From this we conclude that $w_1(x), w_2(x) \in H^1(0,1)$ and $w_1(x), w_2(x) \notin H^2(0,1)$.

To test convergence of the two non-smooth solutions numerically, we need to find $F_1(v)$ and $F_2(v)$ such that $w_1(x)$ and $w_2(x)$ solves (V). We use integration by parts and that $v(0) = 0 = v(1)$ to find $F_j = F(\varphi_j)$,

$$F_j = -\alpha \int_0^1 u_{xx}\varphi_j \, dx + \underbrace{\int_0^1 (bu_x + cu)\varphi_j \, dx}_{=I_j} = -\alpha \underbrace{\left(\int_{K_j} u_{xx}\varphi_j \, dx + \int_{K_{j+1}} u_{xx}\varphi_j \, dx \right)}_{\text{ibp}} + I_j,$$

where we calculate I_j with Simpson's rule and apply i.b.p. for the left integral. Using the fundamental theorem of calculus and simplifying the expression, we get

$$\begin{aligned} F_j &= -\alpha \left(\Big[u_x \varphi_j \Big]_{K_j} - \int_{K_j} u_x \varphi_j' \, dx + \Big[u_x \varphi_j \Big]_{K_{j+1}} - \int_{K_{j+1}} u_x \varphi_j' \, dx \right) + I_j \\ &= \alpha \left(\frac{1}{h_j} \Big(u(x_j) - u(x_{j-1}) \Big) - \frac{1}{h_{j+1}} \Big(u(x_{j+1}) - u(x_j) \Big) \right) + I_j, \end{aligned}$$

which we use to solve (V) for the non-smooth solutions. The resulting convergence plots are shown in Figure 4.

Here we see that the convergence rate of $w_1(x)$ is 1 in both H^1- and L^2-norm, which shows a steady linear convergence even though $w_1(x) \notin H^2$. The fact that the L^2-norm and H^1-norm have the same convergence rate is surprising, as we previously have seen an L^2-convergence of 2. This shows that the theoretical error bound is not applicable to non-smooth functions. For $w_2(x)$ we see that the convergence rates are "random", but steady, with L^2-rate of 0.58 and H^1-rate of 0.174. This shows that we may indeed have convergence even though the solutions are not in H^2.

3.4 Distribution of nodes

Now we turn our attention to the function $f(x) = x^{-\frac{1}{4}}$ to study the effect of the distribution of the nodes. First, we have to confirm $f(x) \in L^2(0,1)$. Looking at the integral we find

$$\int_0^1 |x^{-\frac{1}{4}}|^2 dx = \int_0^1 x^{-\frac{1}{2}} dx = 2 \left[x^{\frac{1}{2}} \right]_0^1 = 2.$$

Thus $f(x) \in L^2(0,1)$. Studying the effect of the distribution of the nodes, we expect a distribution that is more dense where the solution changes rapidly (i.e. the derivative/-gradient is big) to be better than a linearly spaced distribution. Consequently we want to set the coefficients α, b, c and the RHS f such that the solution is steep near 0. We use the f defined above since this choice of $f(x)$ has the property $\lim_{x \to 0^+} x^{-\frac{1}{4}} = \infty$, and the f is a "source term". Also we choose $\alpha = 0.1, b = -5, c = 126$ to obtain this. We want b to be negative since this is the fluid velocity and this way we force it towards 0. α is chosen more or less randomly while c is chosen such that we still fulfill the coercivity. The numerical solution is shown in Figure 6.

For the distribution that is not equispaced, we do an exponential transformation to make them more dense near zero. the details are shown in Figure 7 and Figure 8 in the appendix. To check the error, we do a similar analysis as earlier, and compare with an exact solution for different M. This time we do not have an analytic solution, and therefore use a very refined grid as our "exact" solution. The results are shown in Figure 5. As can be seen by Figure 5, the solution using the "exp"-distributed nodes has a lower error, as expected. This result is consistent for different values of M.

4 Summary

In this project, we have analysed a 1d stationary convection diffusion problem. By the use of the Lax-Milgram theorem, we concluded with the existence of a unique solution. Having done this analysis, we implemented a finite element method and applied it to our problem to find a numerical solution. Here we used a Galerkin approximation to end up with a system of linear equations. Comparing with some chosen sufficiently smooth solutions, we concluded that our method had a convergence rate of 2 in the L_2 norm, and 1 in the H_1 norm. This was consistent with the analytically derived error bound. We then tested our method for some non-smooth exact solutions, and once again looked at the convergence rate. Here we found that the error bound we found for sufficiently smooth functions does not hold for non-smooth functions. Still, our method seemed to converge as we refined our grid. Finally, we confirmed that having a high node density where the function changes rapidly, will significantly reduce the error.

Appendix: Plots

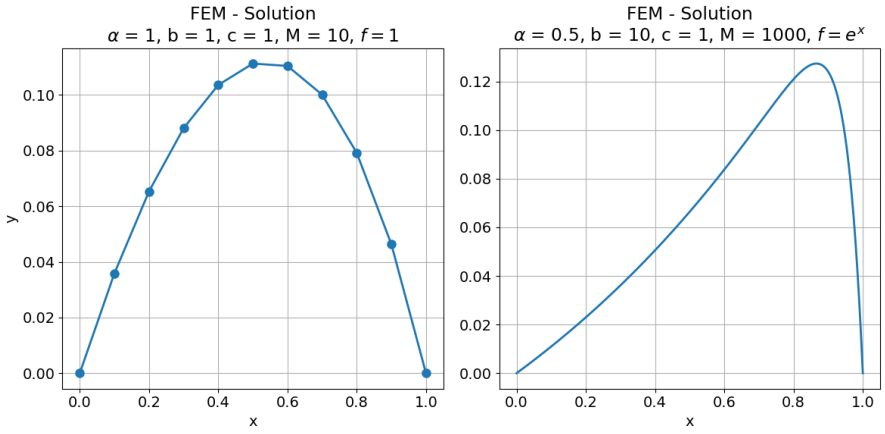

Figure 2: Two solutions of (V_h) for different parameters/RHS's given in title.

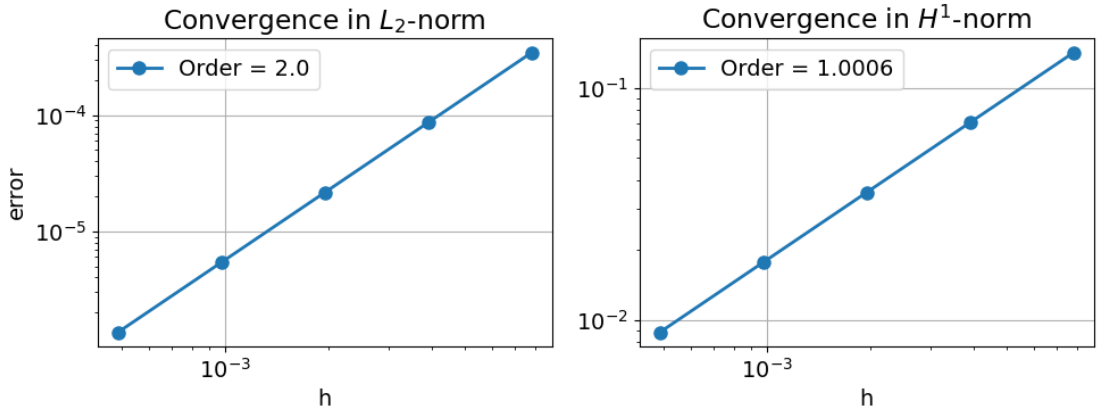

Figure 3: Result of convergence test using $u(x) = \sin(3\pi x)$.

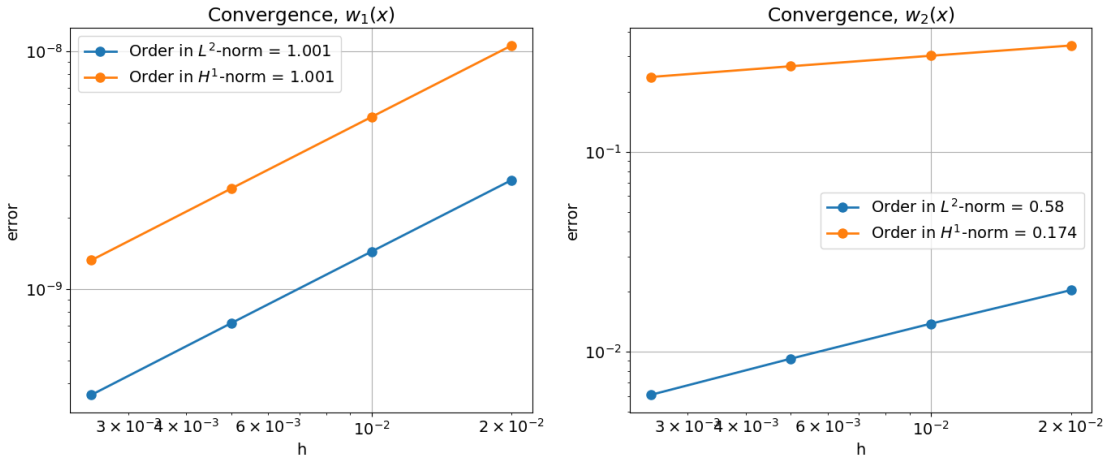

Figure 4: Convergence rates in H^1 and L^2 for the two non-smooth solutions $w_1(x)$ and $w_2(x)$.

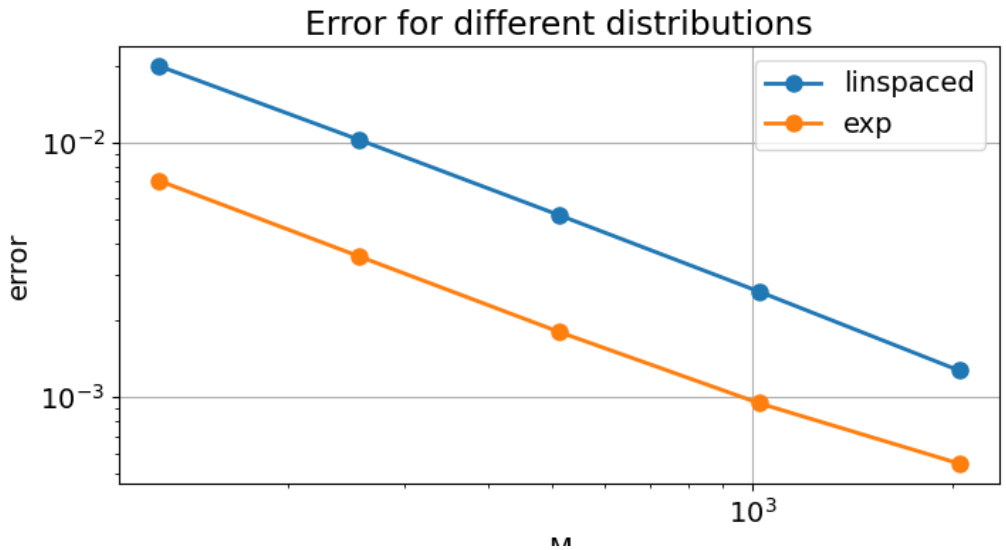

Figure 5: Error for different distribution of nodes. The meaning of the "exp" distribution is explained in the appendix. The errors are calculated in the H^1 norm.

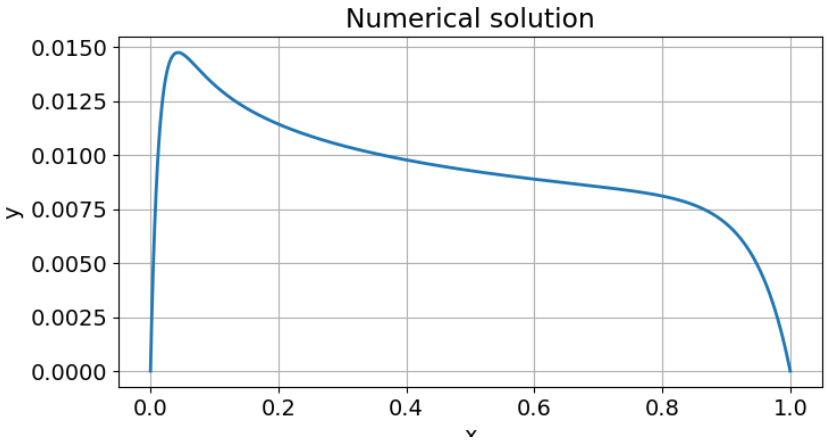

Figure 6: Numerical solution given parameters and RHS given in section 3.3.1. The solution is steep near $x = 0$.

```
def generate_exponential(x0, xend, M):
    x = np.linspace(-1, 1, M)
    y = np.exp(x)
    x = (y - np.min(y)) / (np.max(y) - np.min(y)) * (xend - x0) + x0
    return x
```

Figure 7: Code used to generate the "exp" node distribution.

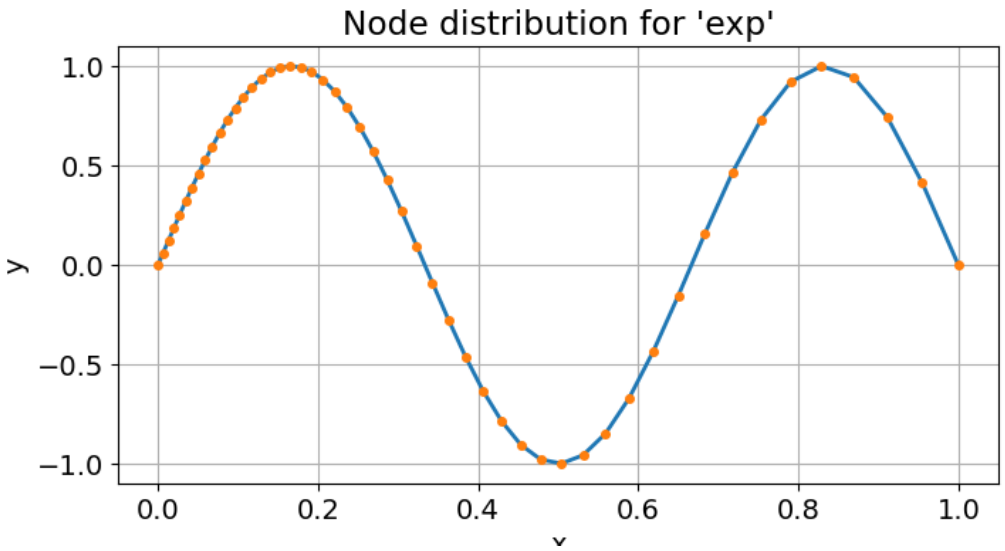

Figure 8: Result of using the ”exp” node distribution with M = 50.

Bibliography

Curry, C. (2018). ‘TMA4212 Part 2: Introduction to finite element methods’. In.